

Short Communication

Improving the Anti-Corrosion Ability of Anodization Film of AZ31B Magnesium Alloy by Addition of NH_4VO_3 in the Electrolyte

Yujun Si^{*}, Zhongping Xiong, Xingwen Zheng, Minjiao Li, Qinhuang Yang

Material Corrosion and Protection Key Laboratory of Sichuan Province, College of Chemistry and Pharmaceutical Engineering, Sichuan University of Science and Engineering, Zigong 643000, P.R. China

*E-mail: syj08448@163.com

Received: 18 December 2015 / Accepted: 8 March 2016 / Published: 1 April 2016

AZ31B magnesium alloy was anodized in an alkaline electrolyte containing sodium borate, sodium silicate and sodium citrate. Ammonium metavanadate (NH_4VO_3) was used as an additive to improve the anti-corrosion ability of anodization film. The anodization film was characterized by X-ray diffraction and scanning electron microscopy. The anti-corrosion ability of the film was evaluated by electrochemical impedance spectrum. The results show that VO_3^- ions react with Mg^{2+} to form yellow magnesium vandate. Magnesium oxide in anodization film is restrained by VO_3^- . The pores on the film decreases and the cracks can be filled by the addition of NH_4VO_3 . The film also becomes smoother and compacter which increase the resistance of film and charge transfer resistance of the corrosion process of the AZ31B magnesium alloy. The anti-corrosion ability of the anodization film is obviously enhanced.

Keywords: Magnesium alloy; anodization film; anti-corrosion; ammonium metavanadate

1. INTRODUCTION

Magnesium alloys are promising structure materials because of its special properties, such as small density, great strength, great stability in size, good casting property, etc. These properties are important in the manufacture of aircraft and automotive industries. Reducing the consumption of fuel and emission of waste gas to protect the environment are urgent in transportation industry. It is recognized as a better choice to reduce the mass of transportation tools by using light structure materials. Magnesium alloys can meet this requirement [1-4]. However, magnesium alloys are active and prone to be corroded, which limits their usage as structure materials [5-7]. So it is necessary to

enhance the anti-corrosion ability of magnesium alloys for their actual applications. Among different methods, surface treatments are commonly employed to deal with this limitation. Electrochemical anodization is an effective surface treatment technique for magnesium alloys [8-12]. The most successful anodization process of magnesium alloys is HAE [13] and DOW17 [14]. The two methods are all superior in both corrosion and abrasion resistance. The shortcoming of the two technologies is that they contain chromate or fluoride and are harmful to environment. So developing a process of chromium-free or/and fluoride-free electrolyte is necessary to the anodization of magnesium alloys. Among these anodization electrolytes, environmental friendly silicate and borate containing system have absorbed researchers' attentions [15-17].

In this study, AZ31B magnesium alloy was anodized in an environmental friendly alkaline electrolyte containing sodium borate ($\text{Na}_2\text{B}_4\text{O}_7$), sodium silicate (Na_2SiO_3) and sodium citrate ($\text{C}_6\text{H}_5\text{Na}_3\text{O}_7$). The ammonium metavanadate (NH_4VO_3) was also added into the electrolyte to investigate its influence on the anodization film.

2. EXPERIMENTAL

AZ31B magnesium alloy was used as the test material, which contains 3 wt% Al and 1 wt% Zn. A disk-shaped specimen with a diameter of 20 mm and a thickness of 8 mm was cut from an alloy rod. The specimen was connected with a copper conductive wire on one side and mounded in epoxy resin with another side exposed as working surface. Prior to anodization, the working surface was orderly polished with SiC emery paper from #200, #400, #600, #800, #1000 to #1200, and rinsed with de-ioned water and acetone. The basic electrolyte consists of 50 g/L of NaOH, 40 g/L of $\text{Na}_2\text{B}_4\text{O}_7 \cdot 10\text{H}_2\text{O}$, 60 g/L of $\text{Na}_2\text{SiO}_3 \cdot 9\text{H}_2\text{O}$, 20g /L of $\text{C}_6\text{H}_5\text{Na}_3\text{O}_7 \cdot 2\text{H}_2\text{O}$. Different concentration of NH_4VO_3 was added into the electrolyte to investigate its effect on the anodization film. The anodization was carried out at a current density of $10 \text{ mA} \cdot \text{cm}^{-2}$ for 15 minutes at 298 K with continuous stirring. A 40 mm×100 mm stainless steel was used as cathode in the anodization.

The surface morphology of the anodization film was examined by scanning electron microscopy (SEM) (VEGA 3 EasyProbe, TESCAN). X-ray diffraction (XRD) pattern was acquired on a DX-2600 X-ray diffractometer with Cu K α radiation ($\lambda=0.15418 \text{ nm}$) at 40 kV and 25 mA.

The anti-corrosion performance of the anodization film was characterized by electrochemical impedance spectrum (EIS). EIS was measured using a CHI760E workstation (CH Instruments) at 298 K in 3.5 wt% NaCl solution. The measurement was carried out at the open circuit potential from 10^5 Hz to 0.1 Hz with a perturbation voltage of 5 mV. A three-electrode cell was used with a saturated calomel electrode (SCE) as the reference electrode, and a platinum sheet as the counter electrode. The AZ31B magnesium alloy electrode was immersed in NaCl solution for 10 minutes before EIS measurement.

3. RESULTS AND DISCUSSION

The concentration of NH_4VO_3 in the basic electrolyte is 0 g/L, 10 g/L, 20 g/L, 30 g/L, 40 g/L and 50 g/L, respectively. Upon the electrolyzer was imposed with $10 \text{ mA} \cdot \text{cm}^{-2}$ current, the anodization

film was immediately formed on the working surface of AZ31B alloy and the resistance of film increased. About initial 30 seconds later, white spark was observed on the working surface, moving over the entire surface. Fig. 1 shows the relation between the spark starting voltage and concentration of NH_4VO_3 . The spark starting voltage increases from 78V to 94V by increasing the concentration of NH_4VO_3 from 0 g/L to 50 g/L. The result indicates that the VO_3^- ions move to the anodic working surface and take part in the formation of film in the anodization process, which can increase the resistance of the film. The participation of VO_3^- ions in the anodization process can also be confirmed by the color of anodization film as shown in Fig. 2. The film obtained in the electrolyte without NH_4VO_3 is gray. With the addition of NH_4VO_3 , the color of film changes to yellow and becomes darker and deeper with increasing the concentration of NH_4VO_3 . The changing color is the result that the VO_3^- ions react with Mg^{2+} ions to form the yellow magnesium vanadate ($\text{Mg}_2\text{V}_2\text{O}_7$).

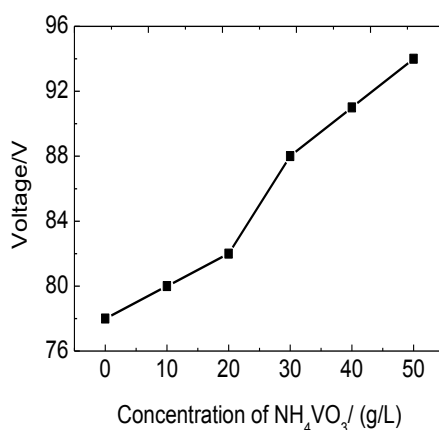


Figure 1. Relation between the spark starting voltage and concentration of NH_4VO_3

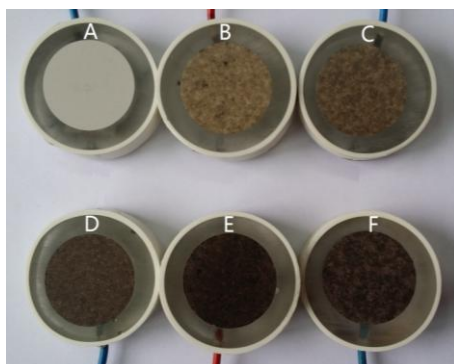


Figure 2. Optical images of anodization films obtained in electrolytes containing different concentration of NH_4VO_3 , (A) 0 g/L, (B) 10 g/L, (C) 20 g/L, (D) 30 g/L, (E) 40 g/L, (F) 50 g/L.

The XRD patterns of anodization films obtained in electrolytes containing 0 g/L and 40 g/L of NH_4VO_3 are shown in Fig. 3. Besides the diffraction peaks of metallic magnesium, strong diffraction peaks of MgO can be found in the anodization film obtained in the basic electrolyte without NH_4VO_3 .

By adding NH_4VO_3 into the electrolyte, just the diffraction peaks of metallic magnesium can be found, and the diffraction peak of MgO disappears. The result further indicates the VO_3^- ions react with Mg^{2+} ions to form a part of anodization film and restrain the formation of MgO . However, the diffraction peaks of the product, yellow $\text{Mg}_2\text{V}_2\text{O}_7$, of VO_3^- ions with Mg^{2+} ions can not be found in the XRD pattern, too. The possible reason is that the $\text{Mg}_2\text{V}_2\text{O}_7$ exists as amorphous state in the anodization film.

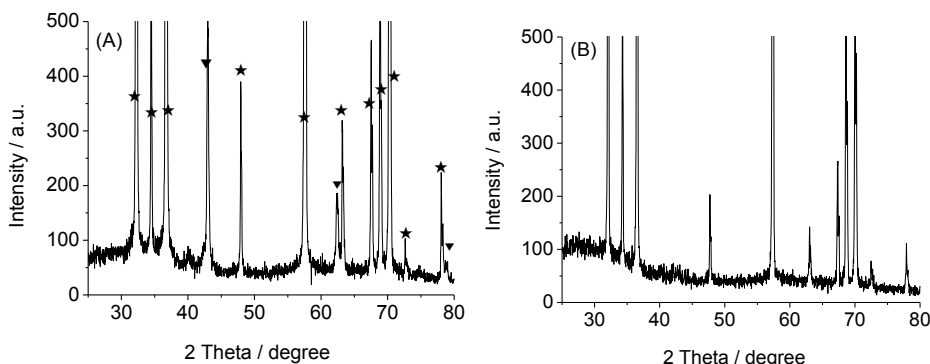


Figure 3. XRD patterns of anodization films obtained in electrolytes containing (A) 0 g/L, (B) 40 g/L of NH_4VO_3 (★: Mg, ▼: MgO).

SEM image of cross-section of specimen anodized in the electrolyte containing 40 g/L of NH_4VO_3 was shown in Fig. 4. The anodization film closed to the magnesium substrate is loose and porous, and then the film become compact which can well protect the magnesium substrate from corrosion. Table 1 lists content of elements in the anodization film by line analysis on the cross-sections of different specimens. It can be found that the boron atom can not be detected in the film. So the $\text{B}_4\text{O}_7^{2-}$ ion may not take part in the formation of the anodization film. On the other hand, the SiO_3^{2-} , $\text{C}_6\text{H}_5\text{O}_7^{3-}$ and VO_3^- ions all move to the surface of magnesium alloy substrate and take part in the formation of the anodization film.

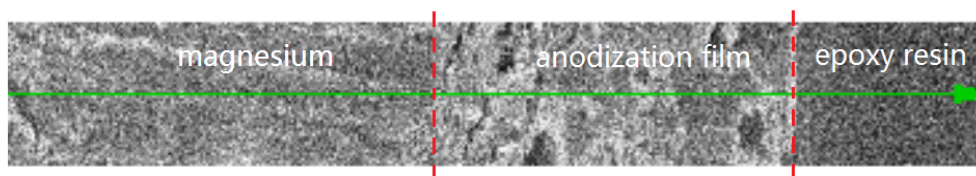


Figure 4. SEM image of cross-sections of specimen anodized in the electrolyte containing 40 g/L of NH_4VO_3

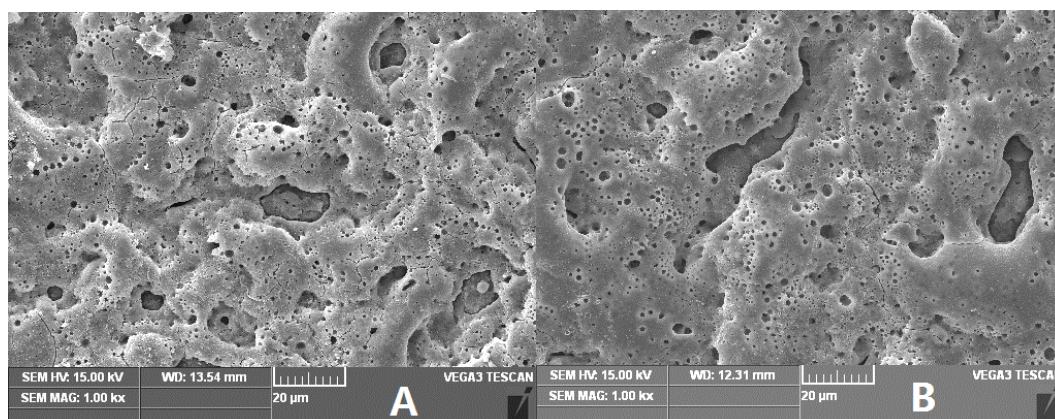
Fig. 5 shows the SEM images of AZ31B alloy surface after anodized in the electrolyte containing various concentrations of NH_4VO_3 . Many pores and cracks can be observed on the surface of the specimen anodized in the electrolyte without NH_4VO_3 . It suggests the density of film consisted of MgO and the SiO_3^{2-} , $\text{C}_6\text{H}_5\text{O}_7^{3-}$ are greater than the magnesium alloy, which is the source of the

crack appearing. However, by the addition of NH_4VO_3 , the amount of the pore decreases and the cracks are filled. The anodization film also becomes smoother. These structures are beneficial to enhance the anti-corrosion performance of the film. A better surface morphology of AZ31B alloy can be obtained at concentrations of 30 g/L to 40 g/L of NH_4VO_3 . Then the anodization film becomes rougher and some big pores appear again at a greater concentration of NH_4VO_3 .

Table 1. Atomic percentage of different elements in the anodization film

Concentration of NH_4VO_3 / g/L	V/ at %	Si/ at %	O/ at %	Mg/ at %	Na/ at %	C/ at %
10	3.86	6.95	42.36	27.81	3.02	16
20	5.75	7.84	43.56	25.42	3.32	14.11
30	7.76	7.53	44.89	22.84	4.37	12.61
40	10.93	7.53	44.04	20.21	5.07	12.22
50	15.17	7.24	44.43	17.09	4.68	11.39

The anti-corrosion ability of the anodization film on AZ31B magnesium alloy was characterized by the EIS technique as shown in Fig. 6. The Nyquist plots of all the tests consist of one semi-circle capacitive loops. The semi-circle can be modeled by a typical equivalent circuit of porous films with five elements R_s , R_f , CPE_f , R_{ct} and CPE_{dl} [3,18-21] by ZsimDemo software. Herein, R_s represents the solution resistance; R_f represents the resistance of anodization film; the CPE_f is related to the capacitance of anodization film. R_f and CPE_f reflect the properties of the anodization film. The double layer capacitance (CPE_{dl}) models the characteristic of faradic reaction on the substrate interface; the charge transfer resistance (R_{ct}) can be referred to the anodic dissolution of Mg into Mg^{2+} . Larger R_f indicates the anodization film is compacter, and larger R_{ct} means the anodic dissolution on the substrate becomes more difficult. Table 2 lists the fitting values of R_f and R_{ct} . It can be seen that the values of the two resistance increase by the addition of NH_4VO_3 into the basic electrolyte. The values of R_f and R_{ct} are largest in the electrolyte containing 40 g/L of NH_4VO_3 . Thereby, the anodization film can act as a more effective barrier and effectively protect the AZ31B magnesium alloy from corrosion.



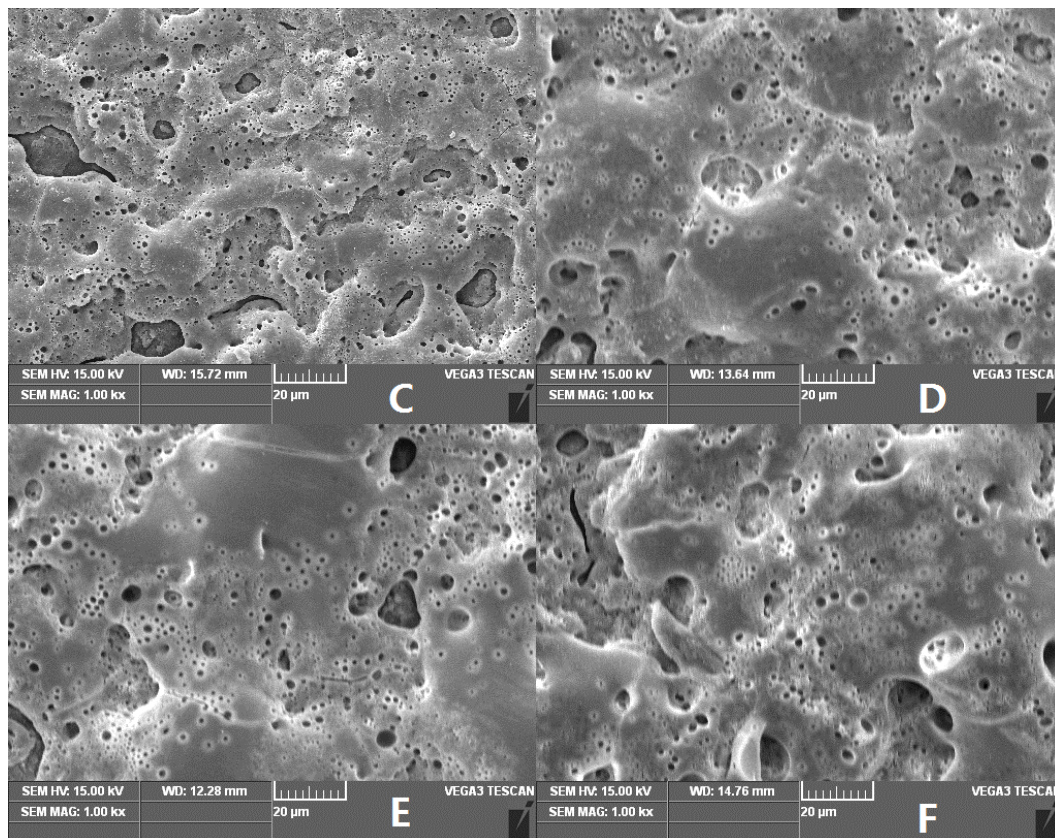


Figure 5. SEM images of anodization films obtained in electrolytes containing different concentration of NH_4VO_3 , (A) 0 g/L, (B) 10 g/L, (C) 20 g/L, (D) 30 g/L, (E) 40 g/L, (F) 50 g/L

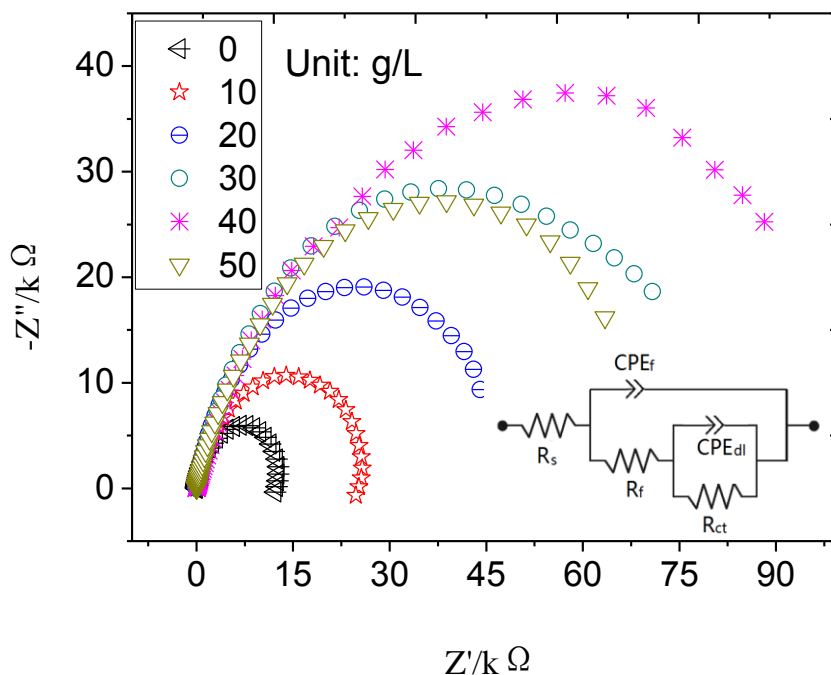


Figure 6. Nyquist plots of the anodization films obtained in electrolytes containing different concentration of NH_4VO_3 and equivalent circuit (inset)

Table 2. EIS fitting results of anodization films obtained in electrolytes containing different concentration of NH_4VO_3

Concentration of NH_4VO_3 / (g/L)	0	10	20	30	40	50
$R_f/(\Omega \text{ cm}^2)$	1873	4101	3652	3529	4355	4283
$R_{ct}/(10^4 \Omega \text{ cm}^2)$	3.701	7.169	12.497	19.405	24.043	17.691

4. CONCLUSIONS

(1) AZ31B magnesium alloy was anodized in an electrolyte containing NH_4VO_3 . VO_3^- ions take part in the formation of anodization film, which increases the film resistance and spark starting voltage in the process.

(2) By the addition of NH_4VO_3 , the number of pores on the film reduces and the cracks can be filled. The anodization film also becomes smoother and compacter.

(3) From the result of EIS test, the anodization film resistance R_f and charge transfer resistance R_{ct} increase by anodizing the AZ31B magnesium alloy in an electrolyte containing NH_4VO_3 . The best anti-corrosion of anodization film can be obtained at a concentration of 30-40 g/L of NH_4VO_3 .

ACKNOWLEDGMENTS

This work was supported by the Opening Project of Material Corrosion and Protection Key Laboratory of Sichuan province (No: 2013CL14, 2014CL07), the Program of Education Department of Sichuan Province (No. 15ZB0208) and the Program of Science and Technology Department of Sichuan province (No. 2014JY0007).

References

1. H.K. Lim, D.H. Kim, J.Y. Lee, W.T. Kim, D.H. Kim, *J. Alloy. Compd.*, 468(2009)308-314.
2. L.Wang, T. Shinohara, B.P. Zhang, *J. Alloy. Compd.*, 496(2010) 500-507.
3. S.Y. Jian, Y.R. Chu, C.S. Lin, *Corros. Sci.* 93 (2015) 301-309.
4. I.A. Kartsonakis, S.G. Stanciu, A.A. Matei, E.K. Karaxi, R. Hristu, A. Karantonis, C.A. Charitidis, *Corros. Sci.*, 100 (2015) 194-208.
5. J. Hirsch, T. Al-Samman, *Acta Mater.*, 61 (2013):818-843.
6. G.L. Song, *Adv. Eng. Mater.*, 7 (2005) 563-586.
7. D. Nam, W.C. Kim, J.G. Kima, K.S. Shin, H.C. Jung, *J. Alloy. Compd.*, 509(2011) 4839-4847.
8. Y. Choia, S. Salman, K. Kuroda, M. Okido, *Corros. Sci.*, 63(2012) 5-11.
9. H.Y. Hsiao, H.C. Tsung, W.T. Tsai, *Surf. Coat. Tech.*, 199(2005) 127-134.
10. L.J. Zhang, J.J. Fan, Z. Zhang, F.H. Cao, J.Q. Zhang, C.N. Cao, *Electrochim. Acta*, 52(2007) 5325-5333.
11. Y. Song, K. Dong, D. Shan, E.H. Han, *J. Magnes. Alloy*, 1(2013)82-87.
12. L.X. Chen, Y. Liu, Z.Y. Liu, X.Y. Zhao, W. Li, *Mater. Corros.*, 66 (2015) 963-970.
13. H.A. Evangelides, *U.S. Pat.* 2723952,1955.11.15.
14. C.C. Dow, *G.B. Pat.* 762195,1956.11.28.
15. W. Li, W. Li, L. Zhu, H. Liu, X. Wang, *Mater. Sci. Eng. B*, 178(2013) 417-424.

16. Y. Liu, Z. Wei, F. Yang, Z. Zhang, *J. Alloy. Compd.*, 509 (2011) 6440-6446.
17. L. Chai, X. Yu, Z. Yang, Y. Wang, M. Okido, *Corros. Sci.*, 50 (2008) 3274-3279.
18. K. Dong, Y. Song D. Shan, E.H. Han, *Corros. Sci.*, 100 (2015) 275-283
19. H.M. Mousa, K.H. Hussein, H.R. Pant, H.M. Woo, C.H. Park, C.S. Kim, *Colloid Surfaces A: Physicochem. Eng. Aspects.*, 488 (2016) 82-92
20. F. El-Taib Heakal, O.S. Shehata, N.S. Tantawy, *Corros. Sci.*, 86 (2014) 285-294
21. S. Yagi, K. Kuwabara, Y. Fukuta, K. Kubota, E. Matsubara, *Corros. Sci.*, 73 (2013) 188-195

© 2016 The Authors. Published by ESG (www.electrochemsci.org). This article is an open access article distributed under the terms and conditions of the Creative Commons Attribution license (<http://creativecommons.org/licenses/by/4.0/>).